Memo 1282

on of St ral ace of C nd otary Applica

Mark S. L

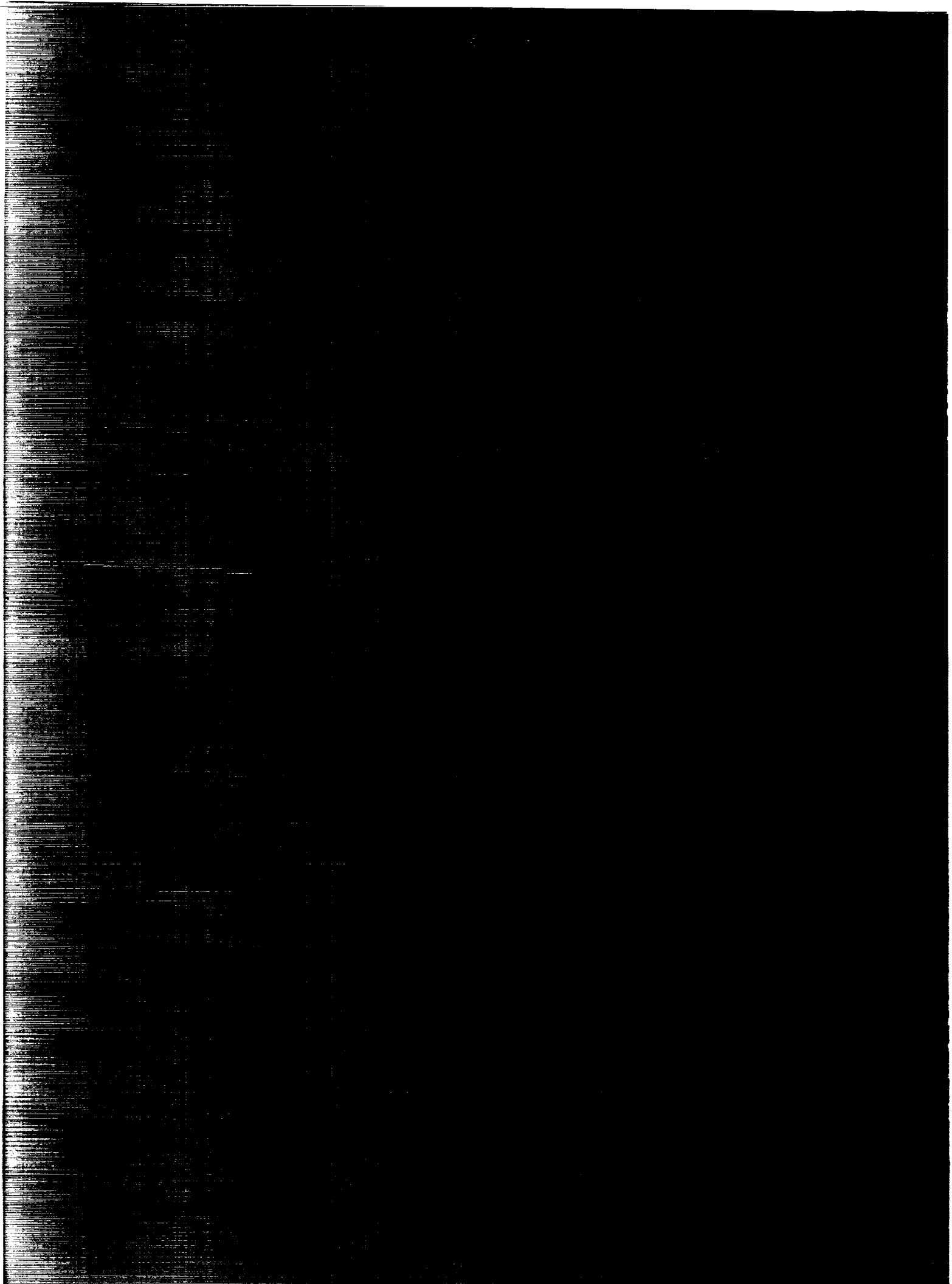

NASA Technical Memorandum 4282

Comparison of Structural Performance of One- and Two-Bay Rotary Joints for Truss Applications

J. Douglas Vail and Mark S. Lake
Langley Research Center
Hampton, Virginia

National Aeronautics and
Space Administration

Office of Management

Scientific and Technical
Information Program

1991

Abstract

This study addresses the structural performance of one- and two-bay large-diameter discrete-bearing rotary joints for application to truss-beam structures such as Space Station *Freedom*. Finite element analyses are performed to determine values for rotary joint parameters that give the same bending vibration frequency as the parent truss beam. The structural masses and maximum internal loads of these joints are compared to determine their relative structural efficiency. Results indicate that no significant difference exists in the masses of one- and two-bay rotary joints. This conclusion is reinforced with closed-form calculations of rotary joint structural efficiency in extension. Also, transition truss-member loads are higher in the one-bay rotary joint. However, because of the increased buckling strength of these members, the external load-carrying capability of the one-bay concept is higher than that of the two-bay concept.

Introduction

The original reference configuration description (ref. 1) for Space Station *Freedom* introduced the concept of a large rotary joint within the truss structure which allows for slewing of the solar arrays. Subsequent developments have established a rotary joint design that occupies one truss bay and incorporates an annular ring with discrete bearings attached to transition truss members. (See fig. 1.) A rotary joint of similar design may be used in a variety of missions following Space Station *Freedom*. An example is the in-space construction facility, which is shown in figure 2 and explained in detail in reference 2. This facility will use rotary joints for solar power system pointing and for slewing of a large space crane (ref. 3) to help position payloads.

An early study of a discrete-bearing rotary joint (ref. 4) determined that the structural efficiency of the joint is highly dependent on the ring diameter and transition truss-member length; the structural efficiency is defined as the ratio of the joint stiffness (i.e., extensional, bending, or torsional) to the joint mass. Because of the operational considerations identified in reference 5, the rotary joint should occupy an integral number of bay lengths of the parent truss beam, that is, the truss beam to which the rotary joint is attached. Therefore, only geometries occupying one- and two-bay lengths are currently being considered. A recent study (ref. 6) addressed the effect of ring diameter in a two-bay rotary joint. This study showed that the total mass of the rotary joint can be minimized by using a ring diameter nearly as large as the depth of the parent truss beam.

The purpose of the present study is to compare the masses of one- and two-bay rotary joints for a range of ring diameters. As a criterion, the vibration frequencies of a portion of truss that includes the rotary joint should be greater than or equal to that of a similar portion of truss with no rotary joint. Therefore, the relative efficiencies of different rotary joints are determined by comparing their structural masses. The bending and torsional frequencies are determined by using finite element analysis of the free vibration in a portion of the Space Station *Freedom* structure that contains the rotary joint. The extensional efficiency of these rotary joints is analyzed in closed form and presented in the appendix to provide qualitative support to the finite element analysis. Also, internal loads are determined for statically applied external bending and torsional moments, and the results are compared for the rotary joint concepts.

Symbols

A	cross-sectional area of transition truss members, in^2
B, C	groups of equal-length transition truss members
d	ring diameter, ft
E	Young's modulus, lb/in^2
f_b, f_t	first bending and first torsion frequencies of structure with rotary joint, Hz
$f_{b,\text{baseline}}$	first bending frequency of structure without rotary joint, Hz
$f_{t,\text{baseline}}$	first torsion frequency of structure without rotary joint, Hz
l	base width of transition truss, ft
M	total mass of transition truss, lbm
n	$= B, C$
P	extensional load of transition truss, lbf
P_{cr}	Euler buckling load of transition truss members, lbf
P_{max}	maximum transition truss-member compression load, lbf
P_n	component of load in member n along direction of displacement, lbf
$\overline{P}_n$	loads in member n of transition truss, lbf
t	thickness of cross section of annular ring, in.
α	rotation angle of rotary joint, deg

β_n	dimension parameter for member n (see fig. A2)
γ	ratio of transition truss length to its base width
δ_n	extension in member n of the transition truss, in.
ρ	material density of transition truss, lbm/in^3
Ω	ratio of transition truss extensional stiffness to mass, lbf/lbm

Concept Definition

The rotary joint consists of an annular ring connected to the truss beam by 12 transition truss members inboard and 12 members outboard of the ring. (See fig. 3.) Three transition truss members connect each node on the end face of the parent truss beam with three points on the ring separated by 45°. This pattern is repeated four times around the ring to form an octagon of attachment points. The inboard transition members are connected directly to the ring, and the outboard transition members are connected to eight discrete-bearing assemblies. These bearing assemblies are mounted to a bearing track on the ring and interconnected by cross-tie members that maintain spacing and transmit circumferential loads between assemblies. The bearing assemblies transmit radial and thrust loads to the ring. The thrust loads are normal to the plane of the ring.

The structural characteristics of the discrete-bearing rotary joint change with rotation angle α as shown in figure 4. For $\alpha = 0°$ and multiples of 45°, the transition truss-attachment points align across the ring; thus, member loads pass directly across the ring. However, for all other rotation angles, the transition truss-attachment points do not align across the ring, so load transfer causes bending and torsion of the ring. Therefore, the ring should be designed with sufficient stiffness to minimize variation in the equivalent stiffness of the rotary joint with rotation angle.

To maintain the performance of the parent truss beam, the equivalent stiffness of the rotary joint should be greater than or equal to that of the parent truss beam. However, since it is difficult to derive explicit values for equivalent bending and torsional stiffness, this criterion requires that the bending and torsional vibration frequencies of a portion of the truss structure that contains the rotary joint are greater than or equal to those of an equivalent structure with no rotary joint. Therefore, the analysis is reduced to sizing the ring with adequate stiffness for the frequencies to be essentially invariant with rotation angle and determining the transition truss-member stiffness that provides adequate rotary joint stiffness for a given ring diameter. Finally, the relative efficiencies of different rotary joints can be determined by comparing their structural masses.

Description of Finite Element Models

The structural performance of the rotary joint concepts is evaluated with finite element models developed by using the Engineering Analysis Language (ref. 7). These models (fig. 5) represent one-half of the Space Station *Freedom* truss structure or the span from the tip of the transverse boom to the center of the module cluster (fig. 1) and consist of fourteen 5-m truss bays. One model is constructed without a rotary joint, and the other two models contain a one- and two-bay rotary joint, respectively. The model without the rotary joint is used to determine baseline vibration frequencies of the transverse boom. All models are cantilevered at the end that corresponds to the center of the module cluster, and the rotary joint is assumed to be locked to prevent rotation.

Information on structural components and attached masses for these models was derived from unpublished preliminary design data for Space Station *Freedom*. The truss members are modeled with only axial stiffness and sized to represent graphite/epoxy tubes with a thin, adhesively bonded outer layer of aluminum. The tubes are 2 in. in diameter with a cross-sectional area of 0.5 in^2, a Young's modulus of 14.4×10^6 psi, and a density of 0.065 lbm/in^3. The truss nodes have a mass of 10.5 lbm each, which is represented by concentrated masses within the model.

The solar arrays and radiators are modeled as rigid beams with masses of 670 lbm and 518 lbm; these beams are assumed to be rigid to eliminate local vibration. The solar-array mass is divided into two parts with half placed at each end. The radiator mass is similarly divided between its two end points. These solar arrays and radiators are attached to four nodes on the face of the truss by rigid beams as shown in the inset of figure 5. An additional mass of 76 lbm is placed at the base of each solar array to represent the deployment cannister, and a mass of 2380 lbm is placed at the base of each radiator to represent the power management and distribution module.

The rotary joint transition truss members are assumed to have the same material properties as the transverse boom truss members, and their cross-sectional area is varied in the study. Although the design of the annular ring is beyond the scope of the present study, a detailed ring analysis presented in reference 6 indicated that a 6-in-square aluminum

cross section with a prescribed thickness provides an estimate of ring size for mass calculations. This thickness is also determined in the study. The outboard transition truss members are attached to the annular ring by linear springs, which represent the bearing assemblies. The stiffness of these springs is assumed to be very large (10^7 lbf/in.) and thus has no effect on the vibration of the structure. These springs are included because they permit direct evaluation of loads in the bearing assemblies.

Discussion of Results

The performance of one- and two-bay rotary joints in bending and torsion is analytically evaluated as a function of ring thickness, ring diameter, and transition truss-member axial stiffness. The first bending and first torsion frequencies of the structure are derived from finite element analysis and plotted for ranges of these variables. Rotary joints that provide the same vibration frequency as the structure without a rotary joint are considered acceptable. For all geometries studied, the lowest two vibration frequencies corresponded to bending in two planes, and the third lowest frequency corresponded to torsion.

Annular Ring Thickness

Variations in the truss vibration frequencies as a function of the rotation angle are caused primarily by annular ring flexibility. As shown in reference 6, a ring cross section sized for the largest ring diameter would be adequate for smaller diameter rings. Because of the payload envelope limitation of the shuttle cargo bay, the maximum practical ring diameter is assumed to be 14 ft. Therefore, the thickness of the annular ring is selected from the comparison of vibration frequency at $\alpha = 0°$ and $\alpha = 22.5°$ for models with ring diameters of 14 ft and transition truss members that have an area and modulus equal to those of the nominal truss struts ($EA = 7.2 \times 10^6$ lbf).

Figures 6(a) and 6(b) show the first bending frequency and first torsion frequency as functions of the thickness of the annular ring for the one- and two-bay rotary joints, respectively. For ring thicknesses larger than 0.05 in., little change occurs in the frequencies. Therefore, an annular ring thickness of 0.05 in. was chosen for all subsequent analyses.

Effect of Transition Truss-Member Stiffness and Ring Diameter

The length of each transition truss member and the angle that each member makes with the plane of the ring are increased as the ring diameter is decreased. This effect causes a loss in stiffness in the rotary joint that must be overcome by increasing the extensional stiffness (cross-sectional area) of the transition truss members. An acceptable rotary joint requires a combination of ring diameter and transition truss-member stiffness that provides frequencies greater than or equal to those of the truss with no rotary joint.

The first bending frequencies for the one- and two-bay rotary joint concepts are plotted in figures 7(a) and 7(b) as functions of the ring diameter and transition truss-member cross-sectional area. The frequencies are normalized to the first bending frequency of the structure without a rotary joint ($f_{b,\text{baseline}} = 0.27$ Hz). The first torsion frequencies for the one- and two-bay rotary joint concepts (figs. 7(c) and 7(d)) are normalized to the first torsional frequency of the structure without a rotary joint ($f_{t,\text{baseline}} = 0.46$ Hz). Comparing figures 7(a) with 7(c) and 7(b) with 7(d), it is impossible to select combinations of ring diameter and transition truss-member cross-sectional area which provide both the first bending and first torsion frequencies equal to the baseline values. These combinations are impossible because a rotary joint that matches the parent truss-bending stiffness has a higher torsional stiffness than the parent truss. Thus, we need to require only that the bending stiffness of the rotary joint match that of the parent truss, and that the torsional stiffness is higher than necessary.

Acceptable combinations of ring diameter and transition truss-member cross-sectional area are derived from figures 7(a) and 7(b) by locating points on the 1.0 normalized frequency line. For example, an acceptable one-bay rotary joint with a ring diameter of 10 ft would be derived from figure 7(a) by following the curve for the ring diameter of 10 ft until it intersects the 1.0 normalized frequency line and then interpolating to find the correct cross-sectional area. For this particular case, an appropriate area is about 1.27 in^2. Table I summarizes necessary transition truss-member cross-sectional areas for both one- and two-bay rotary joints.

Rotary Joint Structural Mass

The total structural mass of the rotary joint can be calculated using the transition truss cross-sectional area and the ring diameter given in table I. Nonstructural masses, such as bearing assemblies, thermal control, and power transfer hardware, are essentially independent of the concept and are thus ignored for comparison purposes. Although the two-bay rotary joint displaces an extra bay from the truss beam as shown in figure 8, it eliminates four nodes from the truss beam that must be replaced using an

Table I. Transition Truss-Member Cross-Sectional Area

Ring diameter, ft	Transition truss-member area, in^2	
	One-bay rotary joint	Two-bay rotary joint
8	3.70	1.55
9	2.00	1.10
10	1.27	.81
11	.83	.60
12	.65	.48
13	.49	.38
14	.38	.31

ancillary structure to allow for mobile transporter operations (ref. 5). The mobile transporter is a utility vehicle that attaches to the truss nodes and moves along the truss beam in one-bay increments.

Since this ancillary structure is undefined, its mass is impossible to calculate. However, this structure should be no more massive than a single bay of truss (138.4 lbm). If the ancillary structure is assumed to have this mass, then the relative efficiencies of the one- and two-bay rotary joints can be evaluated by simply comparing the sums of their ring and transition truss masses.

Structural mass variations for the one- and two-bay rotary joint components are shown as functions of ring diameter in figures 9(a) and 9(b). Since the ring cross section is fixed, its mass is proportional to its diameter. The total mass of the rotary joint is dominated by the mass of the transition truss, and both masses decrease dramatically with increasing ring diameter. A comparison of the total structural mass for the one- and two-bay rotary joints is shown in figure 10. This graph shows that very little difference exists in the total mass of these two joint concepts for ring diameters greater than 10 ft. This result is reinforced by closed-form calculations, presented in the appendix, which show that the most efficient transition truss length for extensional loading is between the lengths of the one- and two-bay rotary joints, and the masses of these two joints are approximately the same.

The importance of the error in estimating the ancillary structure mass for the two-bay rotary joint can be evaluated by using figure 10. If the actual mass of this structure is below the assumed value of 138.4 lbm, then the total mass curve for the two-bay joint should be lowered by the difference in these values. This curve can be lowered 50 to 75 lbm without causing the two-bay rotary joint to become significantly more efficient than the one-bay concept. Thus, no significant difference exists in the efficiency of these two concepts for any reasonable assumption of the mass of the ancillary structure.

Maximum Internal Forces in Rotary Joint

To complete the comparison of structural performance of the one- and two-bay rotary joints, the load distributions within the joints must be studied to determine their relative load-carrying capabilities. The primary loads in the Space Station *Freedom* structure are due to transient response to external forces. Because of the constraint that all rotary joints have the same stiffness as the parent truss and the conclusion that the masses are not greatly different between the one- and two-bay concepts, the transient response of the structure should be essentially independent of the rotary joint concept. Therefore, a comparison of the load distributions within the rotary joints is based on static bending and torsion moments applied to the structure as shown in figure 11. The magnitude of both these moments is arbitrarily selected to be 2500 ft-lbf.

The maximum transition truss-member compression loads due to the statically applied bending moment are shown in figures 12(a) and 12(b) for the one- and two-bay rotary joints. Also included for comparison are plots of the Euler buckling loads P_{cr} of these members. The maximum member loads that result from the static torsional moment are shown in figures 12(c) and 12(d). The member loads decrease with increasing ring diameter, and the loads are lower in the two-bay rotary joint than those in the one-bay rotary joint. However, the higher member loads in the one-bay rotary joint are offset by the greatly increased buckling strength of the members. This effect is shown in figures 13(a) and 13(b) where the normalized maximum member loads are plotted versus ring diameter for the static bending and torsion moments. These plots show that the one-bay rotary joint experiences lower *normalized* member loads and, thus, is capable of carrying higher external forces than the two-bay rotary joint.

The maximum loads in the bearing assemblies that result from the static bending moment are shown in figure 14. The thrust component of the bearing load is the primary component and is normal to the plane of the ring. The thrust component decreases with increasing diameter and is only slightly greater for the two-bay concept; thus, the thrust component is not a discriminator. The radial

component of the bearing load is a secondary component that arises because the transition truss members are not normal to the ring. This radial component of load is larger for the one-bay rotary joint because of the larger angles between its transition truss members and the direction normal to the plane of the ring. Therefore, the two-bay rotary joint shows a slight advantage over the one-bay concept because of its lower secondary bearing loads.

Concluding Remarks

This study was conducted to determine the structural performance of one- and two-bay rotary joints for application to Space Station *Freedom* and other future missions. The cross section of the rotary joint annular ring was sized with adequate stiffness to minimize variation in the vibration characteristics of the structure as the joint is rotated. Parametric finite element analyses were performed to determine the transition truss-member axial stiffness as a function of ring diameter. These analyses were based on the criterion that the first bending frequency of a portion of the Space Station *Freedom* structure that contains the rotary joint is the same as that of a similar structure without a rotary joint. Results showed no significant difference in the structural masses of the one- and two-bay rotary joints for ring diameters greater than 10 ft.

Finally, a study of the load distribution in the one- and two-bay rotary joints was conducted. Although transition truss-member loads are higher in the one-bay rotary joint, these members have significantly higher buckling strengths; thus, the one-bay rotary joint is capable of carrying higher external forces. Little difference was seen between the thrust component of the bearing load for the two concepts; however, the two-bay concept showed lower radial load components as a result of the shallower inclination angles of its transition truss members. In summary, the one-bay rotary joint concept is considered more attractive because of its higher load-carrying capability and its lack of need for an ancillary structure to replace missing truss nodes.

NASA Langley Research Center
Hampton, VA 23665-5225
June 13, 1991

Appendix

Structural Efficiency of a 12-Member Transition Truss in Extension

The stiffness of the rotary joint is determined, to a great extent, by that of the 12-member transition truss structure. Although it is difficult to determine an explicit expression for the bending stiffness of the transition truss, it is easy to determine one for its extensional stiffness. Determining the structural efficiency of the transition truss in extension should provide insight into its efficiency in bending.

Figure A1 shows the transition truss to be analyzed. It is comprised of members of two different lengths, denoted B and C, and the geometry and extensional displacement of the transition truss are symmetric in each 90° sector around the ring. The base width is l, the truss length is γl, and the diameter of the ring is d. The total load necessary to displace the ring Δ units is P. The ring is assumed to be rigid; thus, all points on the ring move Δ in the axial direction. Because of this, all B members have the same axial load, and all C members have the same load. These member loads are called $\overline{P}_n$ $(n = B, C)$ and can be derived from figure A2, in which the left end of member n is fixed and the right end, which is on the ring, moves an amount Δ to the right. The distance from the left end of the member to a longitudinal line through its ring attachment point is $\beta_n l$; thus, the length of the member is $l\sqrt{\gamma^2 + \beta_n^2}$. The values of β_n, found from the geometry presented in figure A1, are

$$\beta_C = \left(\sqrt{2} - d/l\right)/2 \tag{A1}$$

$$\beta_B = \left[1 + (1 - d/l)^2\right]^{1/2}/2 \tag{A2}$$

The component of $\overline{P}_n$ in the direction of displacement is called P_n, and the value for this component is

$$P_n = \frac{\overline{P}_n \gamma}{\sqrt{\gamma^2 + \beta_n^2}} \tag{A3}$$

With this equation, the extension in the member δ_n can be written as

$$\delta_n = \frac{\overline{P}_n l \left(\gamma^2 + \beta_n^2\right)^{1/2}}{EA} = \frac{P_n l \left(\gamma^2 + \beta_n^2\right)}{EA\gamma} \tag{A4}$$

where EA is the extensional stiffness of the member. The similar triangles in figure A2 can be used to

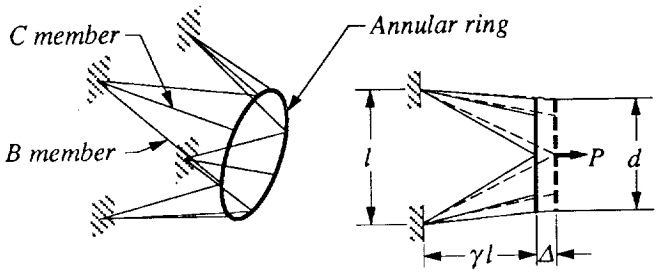

Figure A1. Twelve-member transition truss under extension.

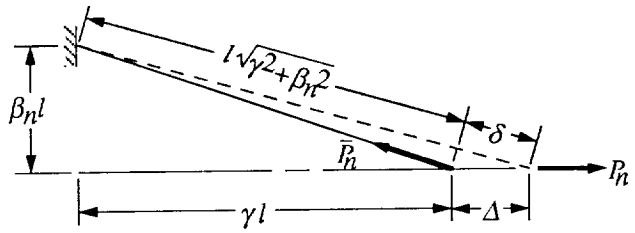

Figure A2. Calculation of member loads for a ring displacement Δ.

relate the truss displacement to the extension in the member by

$$\Delta = \frac{\delta_n \left(\gamma^2 + \beta_n^2\right)^{1/2}}{\alpha} = \frac{P_n l \left(\gamma^2 + \beta_n^2\right)^{3/2}}{EA\gamma^2} \tag{A5}$$

Thus, the load necessary to displace the ring attachment point by an amount Δ is

$$P_n = \frac{\Delta EA\gamma^2}{l\left(\gamma^2 + \beta_n^2\right)^{3/2}} \tag{A6}$$

The total load necessary to displace the ring P is obtained by summing the contributions from eight B members and four C members. The result is

$$P = \frac{4\Delta EA\gamma^2}{l}\left[\frac{1}{\left(\gamma^2 + \beta_C^2\right)^{3/2}} + \frac{2}{\left(\gamma^2 + \beta_B^2\right)^{3/2}}\right] \tag{A7}$$

The equivalent extensional stiffness for the transition truss can be determined from equation (A7) by dividing the load P by the strain $(\Delta/\gamma l)$. Defining the result as EA_{eq} yields

$$EA_{eq} = 4EA\gamma^3\left[\frac{1}{\left(\gamma^2 + \beta_C^2\right)^{3/2}} + \frac{2}{\left(\gamma^2 + \beta_B^2\right)^{3/2}}\right] \tag{A8}$$

The total mass M of the transition truss is found by summing the lengths of all members and multiplying the total by their cross-sectional area A and density ρ as follows:

$$M = 4\rho Al\left[\left(\gamma^2 + \beta_C^2\right)^{1/2} + 2\left(\gamma^2 + \beta_B^2\right)^{1/2}\right] \tag{A9}$$

The efficiency of a structure can be defined as the ratio of its stiffness to its mass. Typically, in a beam-like structure, these quantities are cross-sectional quantities and are thus independent of the beam length. However, in the present study, the mass penalty associated with the rotary joint is considered to be the total joint mass, regardless of whether the joint occupies one or two truss bays. This consideration accounts for the additional structure necessary to maintain all truss nodes in the two-bay rotary joint. Therefore, an efficiency parameter Ω can be defined for the transition structure by dividing the equivalent extensional stiffness presented in equation (A8) by the total truss mass given in equation (A9). The result is

$$\Omega = \frac{E}{\rho l}\frac{\gamma^3\left[2\left(\gamma^2 + \beta_C^2\right)^{3/2} + \left(\gamma^2 + \beta_B^2\right)^{3/2}\right]}{\left(\gamma^2 + \beta_C^2\right)^{3/2}\left(\gamma^2 + \beta_B^2\right)^{3/2}\left[\left(\gamma^2 + \beta_C^2\right)^{1/2} + 2\left(\gamma^2 + \beta_B^2\right)^{1/2}\right]} \tag{A10}$$

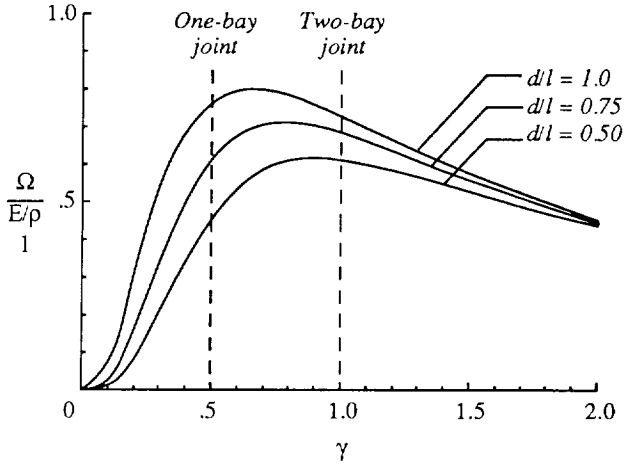

Figure A3. Structural efficiency of 12-member transition truss in extension.

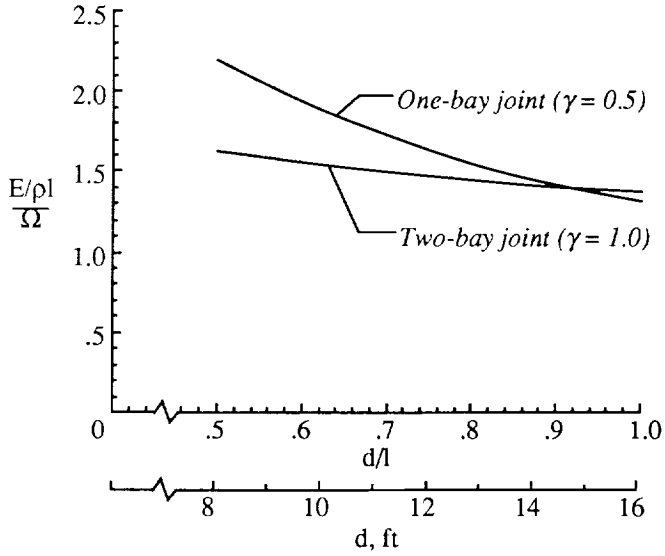

Figure A4. Mass versus ring diameter for one- and two-bay transition trusses.

For a given material and bay length, Ω is a function of only the transition truss length ratio γ and ring diameter ratio d/l. (See eqs. (A1) and (A2).) Figure A3 is a plot of the normalized efficiency versus transition truss length ratio for a series of ring diameter ratios. A one-bay rotary joint is represented by $\gamma = 0.5$, and a two-bay joint by $\gamma = 1.0$. Notice that for the range of ring diameters presented, the transition truss efficiency is maximized for a length between those of the one- and two-bay geometries. The general trend of these curves is similar to the plots of frequency versus transition truss length presented in reference 6. A maximum is present because the efficiency is based on the total truss mass rather than a lineal mass density. For large ring diameters, figure A3 indicates that the one-bay rotary joint is slightly more efficient than the two-bay rotary joint. However, as the diameter is decreased, the member angles of the one-bay rotary joint become large enough to decrease the one-bay efficiency below that of the two-bay geometry.

In the main body of the paper, the structural masses of one- and two-bay rotary joints with the same bending stiffness are plotted versus ring diameter for comparison. A similar comparison, based on extensional stiffness, can be made for one- and two-bay rotary joints by plotting $1/\Omega$ versus d/l for $\gamma = 0.5$ and 1.0 as shown in figure A4. This plot shows the trends previously discussed from figure A3. For small ring diameters, the two-bay rotary joint is less massive (more efficient) than the one-bay rotary joint, but as the ring diameter is increased, the difference in efficiency of the two geometries becomes small. The second abscissa in figure A4 shows the absolute ring diameter based on a 5-m bay size and is included for ease of comparison with results presented in the main body of this report. Figure A4 shows the same qualitative trends obtained by using finite element analysis and considering bending stiffness instead of extensional stiffness. In both cases, little difference exists in the mass (or efficiency) of one- and two-bay rotary joints that have large diameter rings.

References

1. Systems Engineering and Integration Space Station Program Office: *Space Station Reference Configuration Description.* JSC-19989, NASA Lyndon B. Johnson Space Center, Aug. 1984.

2. Mikulas, Martin M., Jr.; and Dorsey, John T.: *An Integrated In-Space Construction Facility for the 21st Century.* NASA TM-101515, 1988.

3. Mikulas, M. M., Jr.; Davis, R. C.; and Greene, W. H.: *A Space Crane Concept: Preliminary Design and Static Analysis.* NASA TM-101498, 1988.

4. Dorsey, John T.; and Bush, Harold G.: *Dynamic Characteristics of a Space-Station Solar Wing Array.* NASA TM-85780, 1984.

5. Mikulas, Martin M., Jr.; Croomes, Scott D.; Schneider, William; Bush, Harold G.; Nagy, Kornell; Pelischek, Timothy; Lake, Mark S.; and Wesselski, Clarence: *Space Station Truss Structures and Construction Considerations.* NASA TM-86338, 1985.

6. Lake, Mark S.; and Bush, Harold G.: *An Analytical Investigation of a Conceptual Design for the Space Station Transverse Boom Rotary Joint Structure.* NASA TM-87665, 1986.

7. Whetstone, W. D.: *EISI-EAL Engineering Analysis Language Reference Manual—EISI-EAL System Level 2091. Volume 1: General Rules and Utility Processors.* Engineering Information Systems, Inc., July 1983.

ORIGINAL PAGE
BLACK AND WHITE PHOTOGRAPH

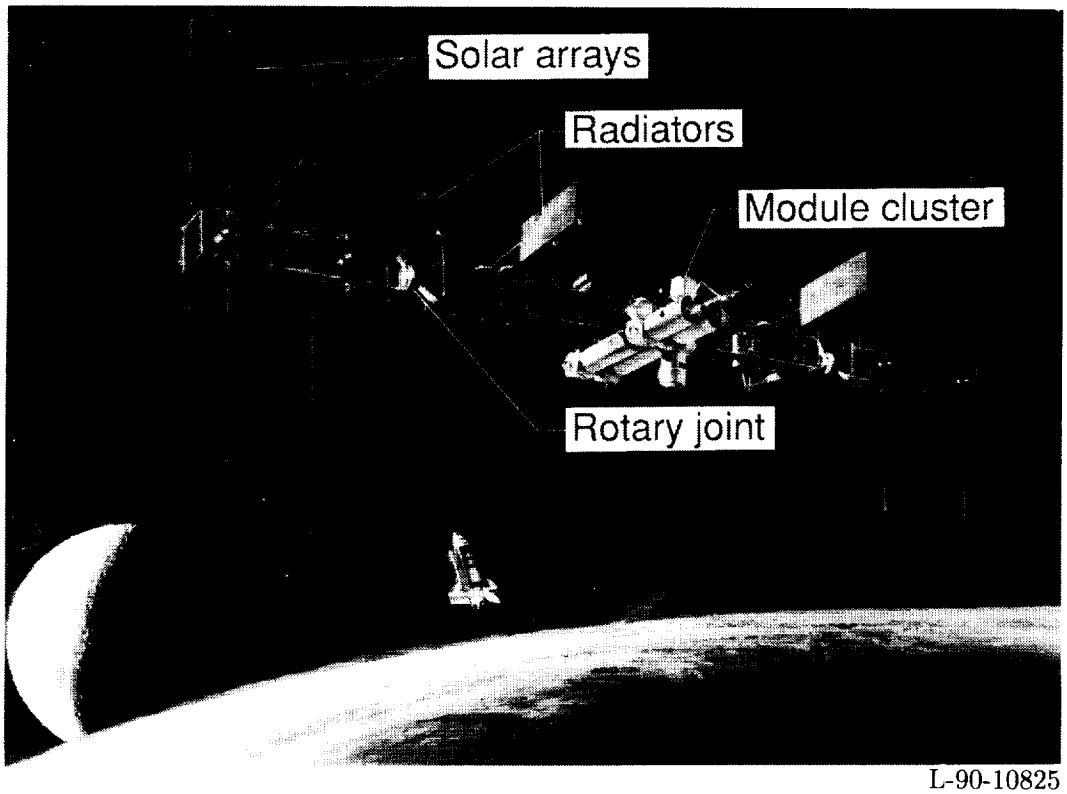

L-90-10825

Figure 1. Space Station *Freedom*.

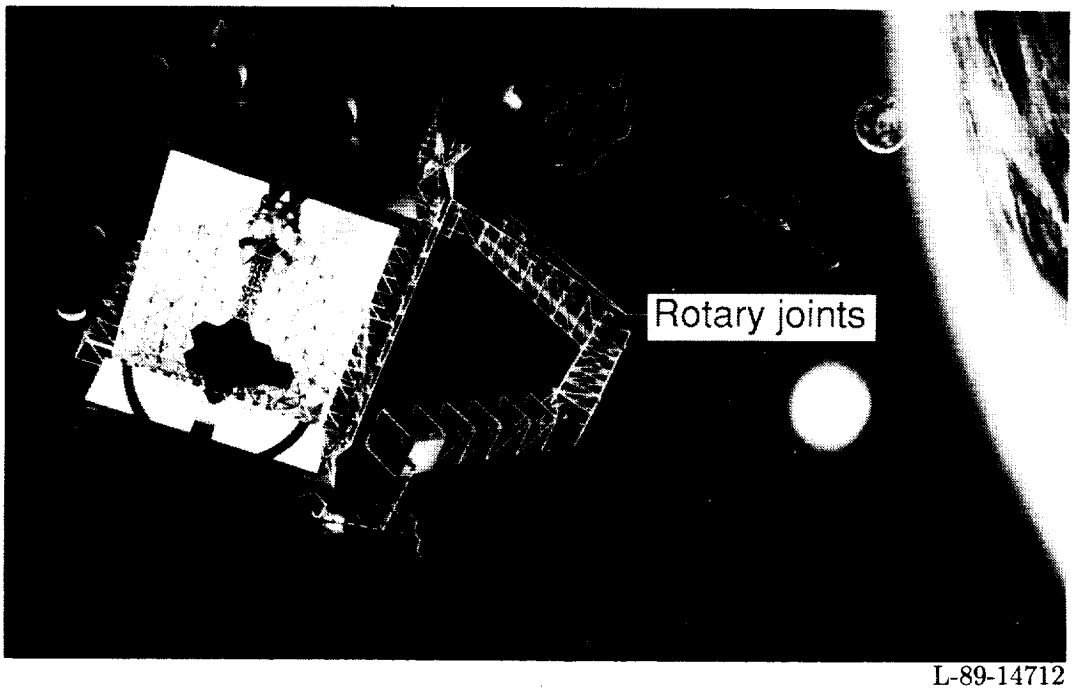

L-89-14712

Figure 2. In-space construction facility and space crane.

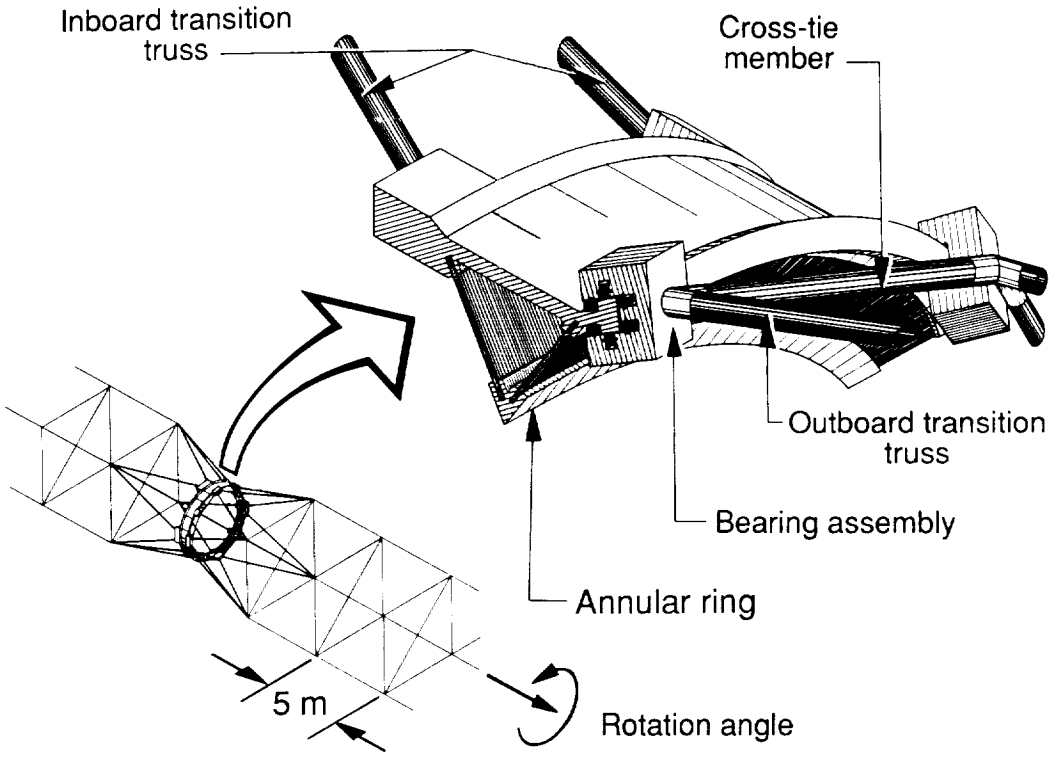

Figure 3. Discrete-bearing rotary joint concept.

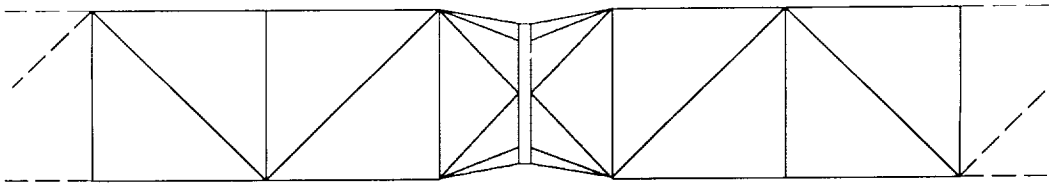

(a) $\alpha = 0°$ (transition truss loads pass directly across ring).

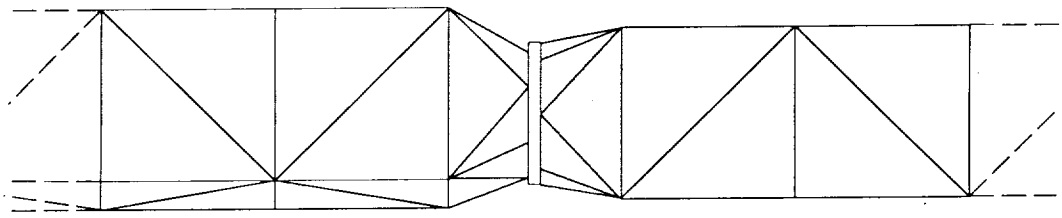

(b) $\alpha = 22.5°$ (transition truss loads cause bending and torsion of ring).

Figure 4. Structural characteristics of discrete-bearing rotary joint.

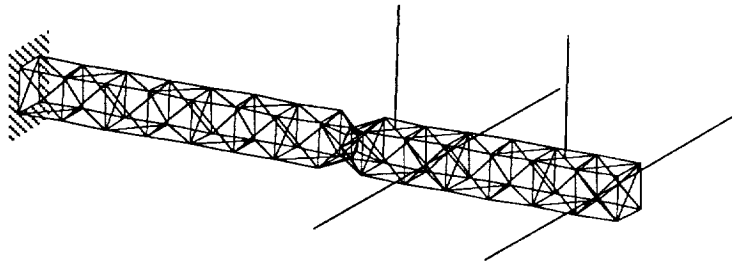

(a) One-bay rotary joint.

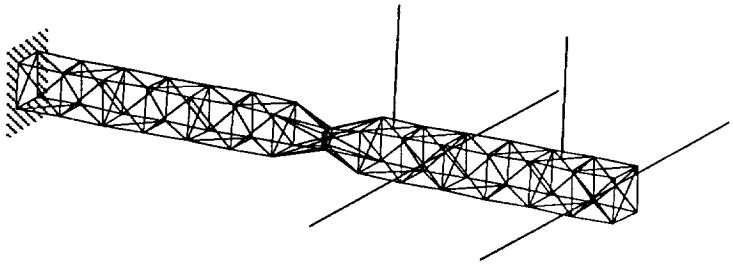

(b) Two-bay rotary joint.

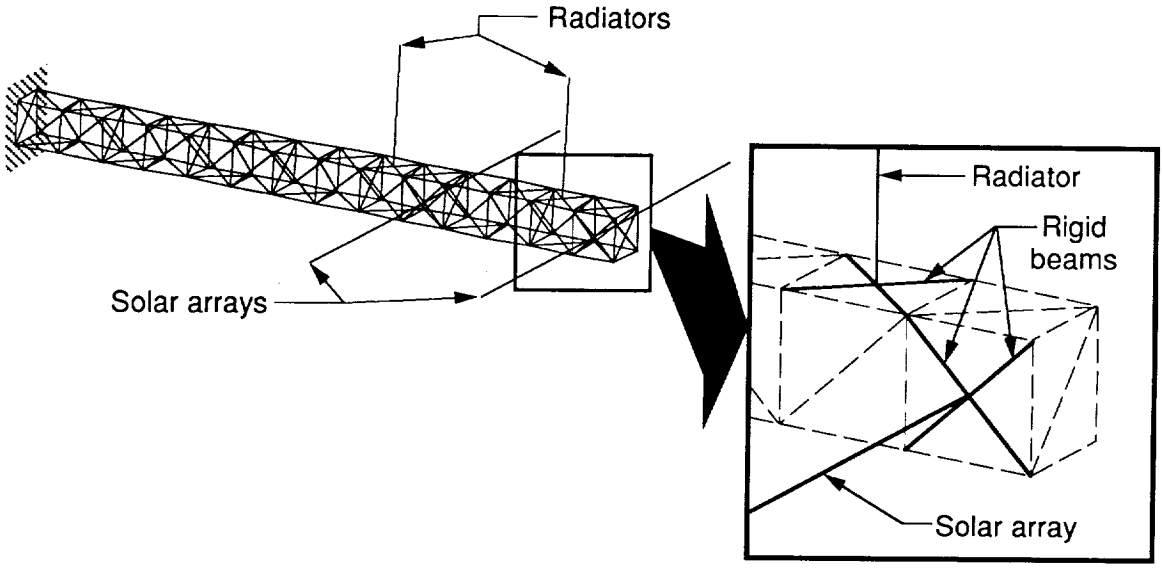

(c) No rotary joint.

Figure 5. Finite element models of one-half of Space Station *Freedom* structure.

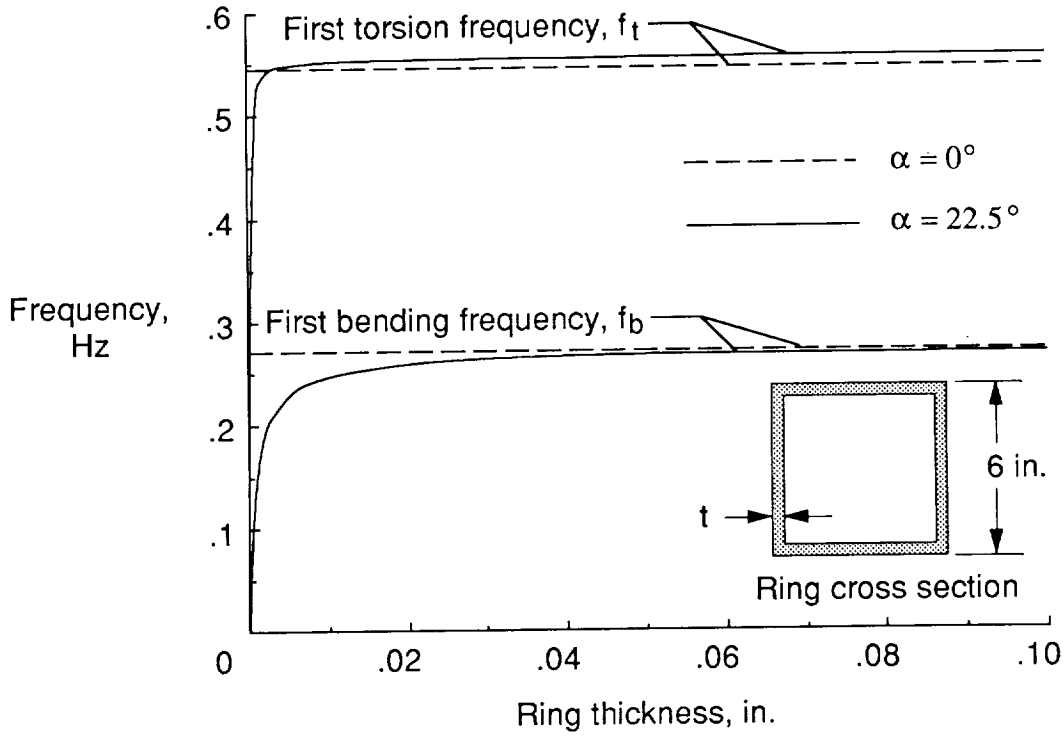

(a) One-bay joint.

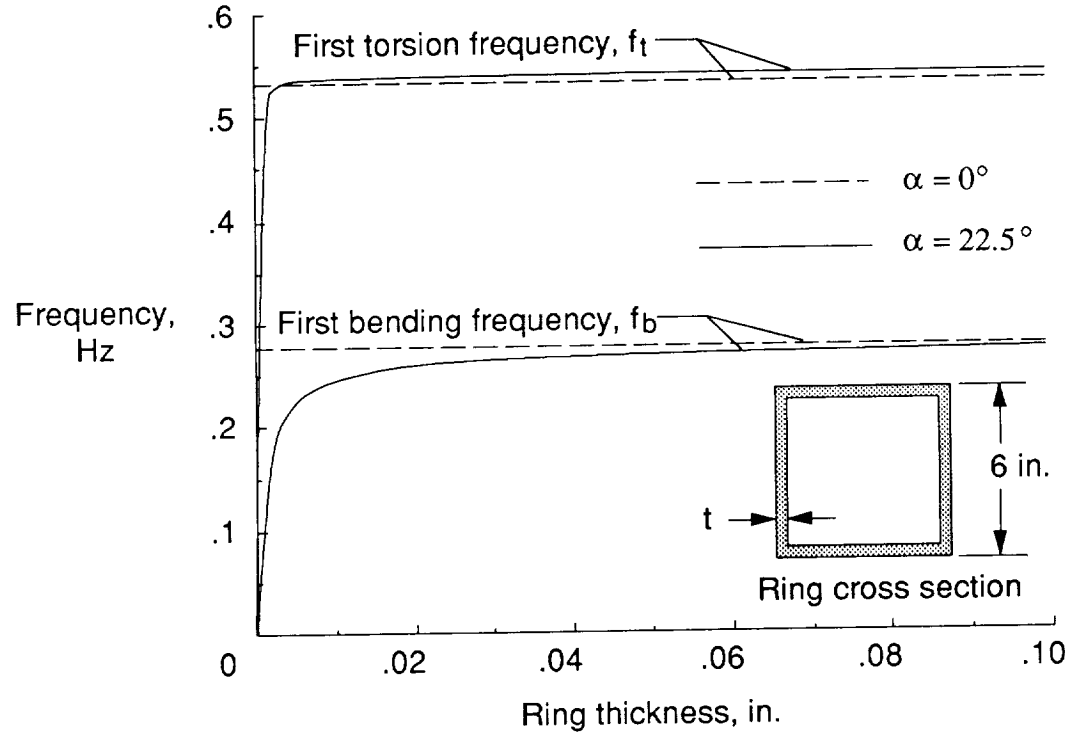

(b) Two-bay joint.

Figure 6. Effect of ring thickness on boom frequencies.

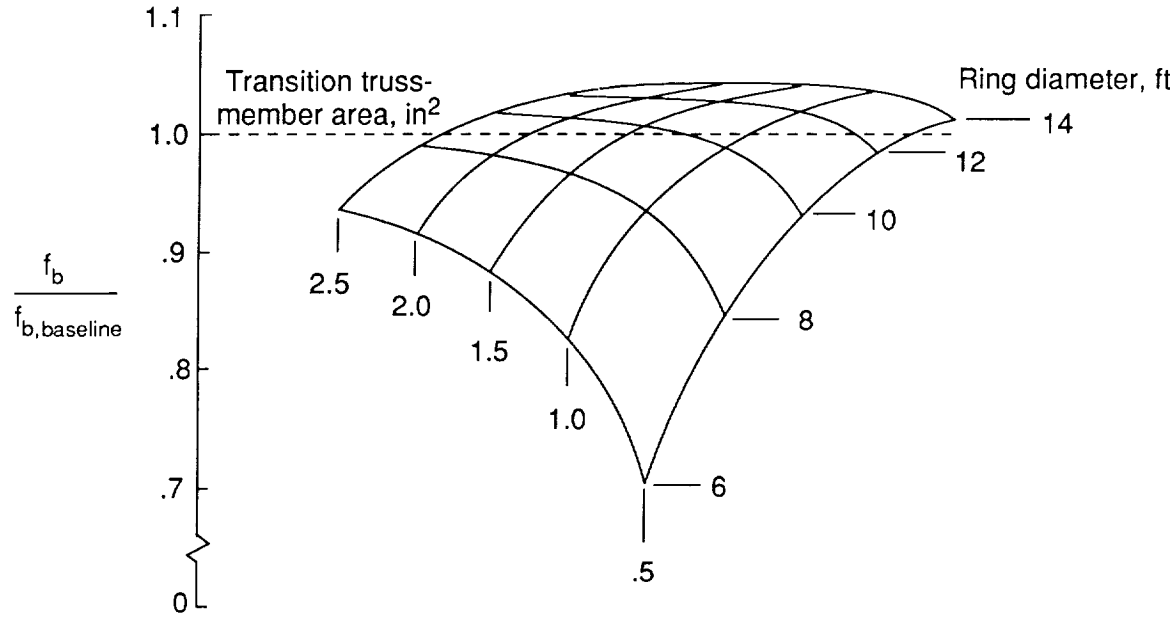

(a) First bending frequency; one-bay joint.

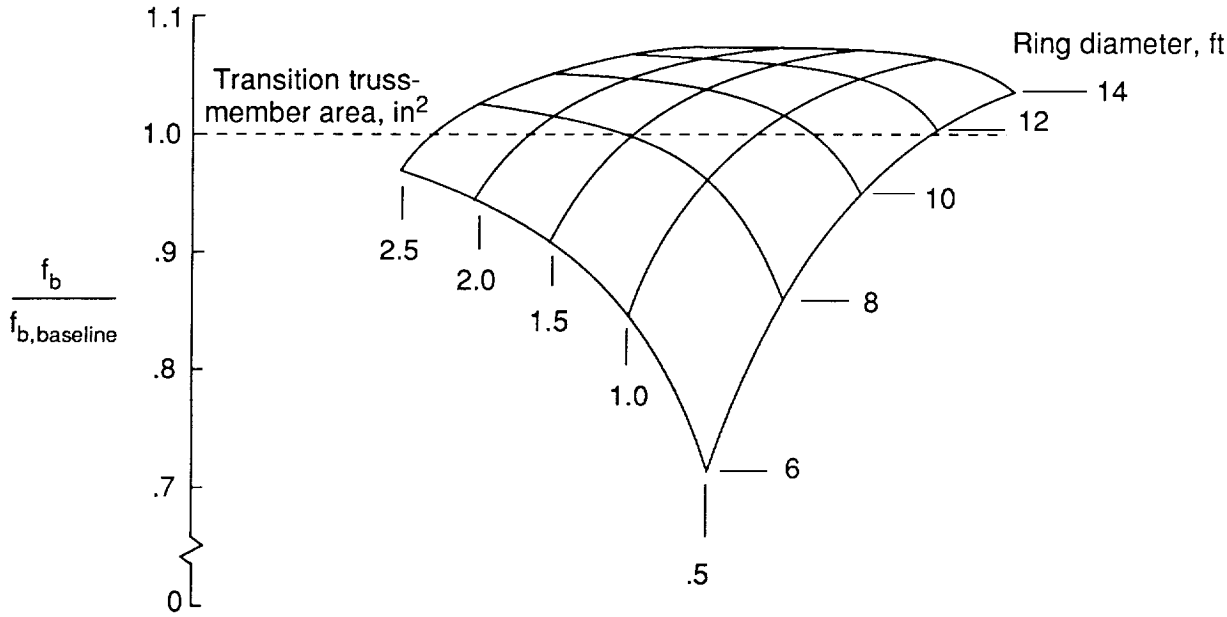

(b) First bending frequency; two-bay joint.

Figure 7. Frequency variation with transition truss-member area and ring diameter.

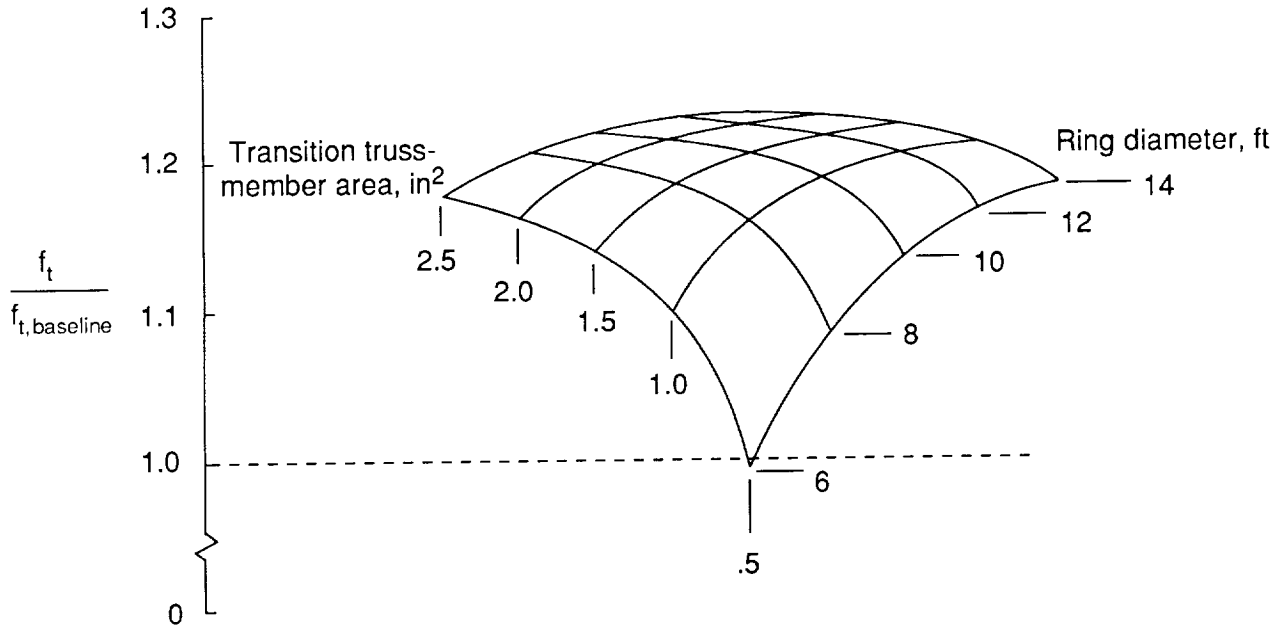

(c) First torsion frequency; one-bay joint.

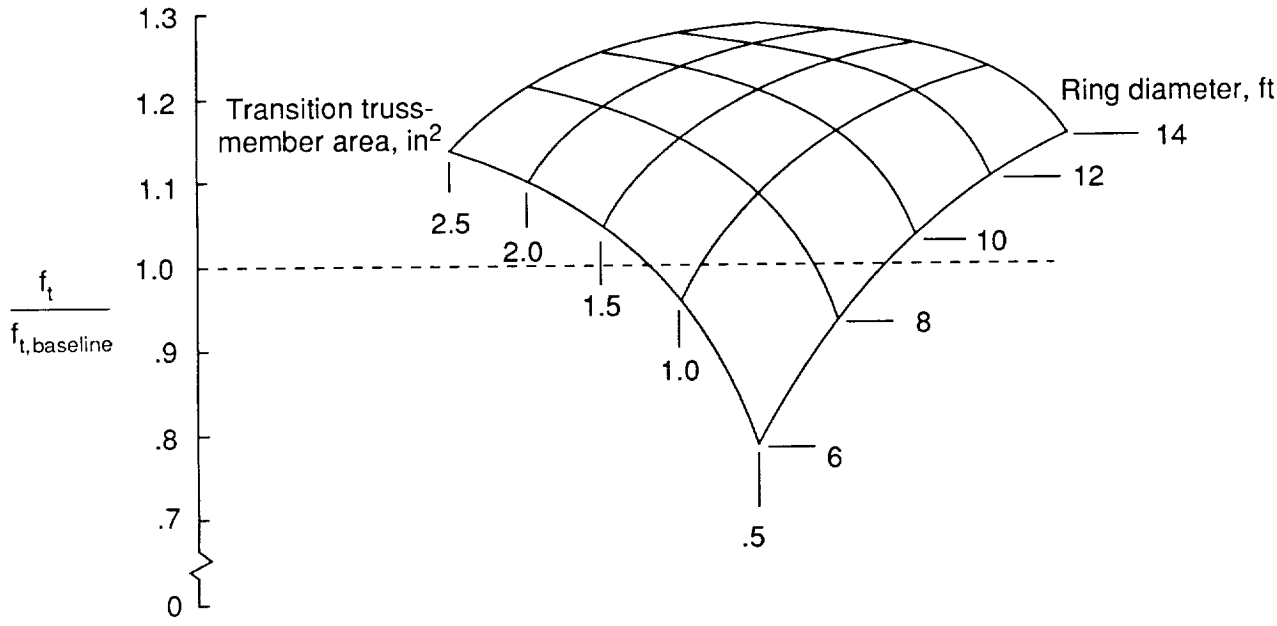

(d) First torsion frequency; two-bay joint.

Figure 7. Concluded.

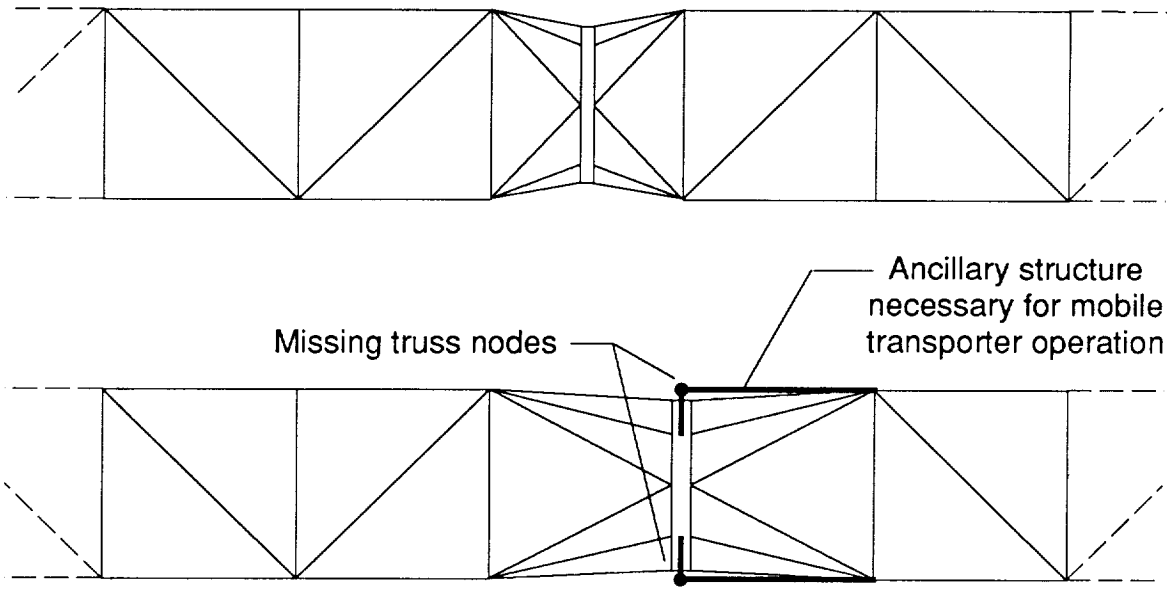

Figure 8. Ancillary structure accounted for in determining mass of two-bay rotary joint.

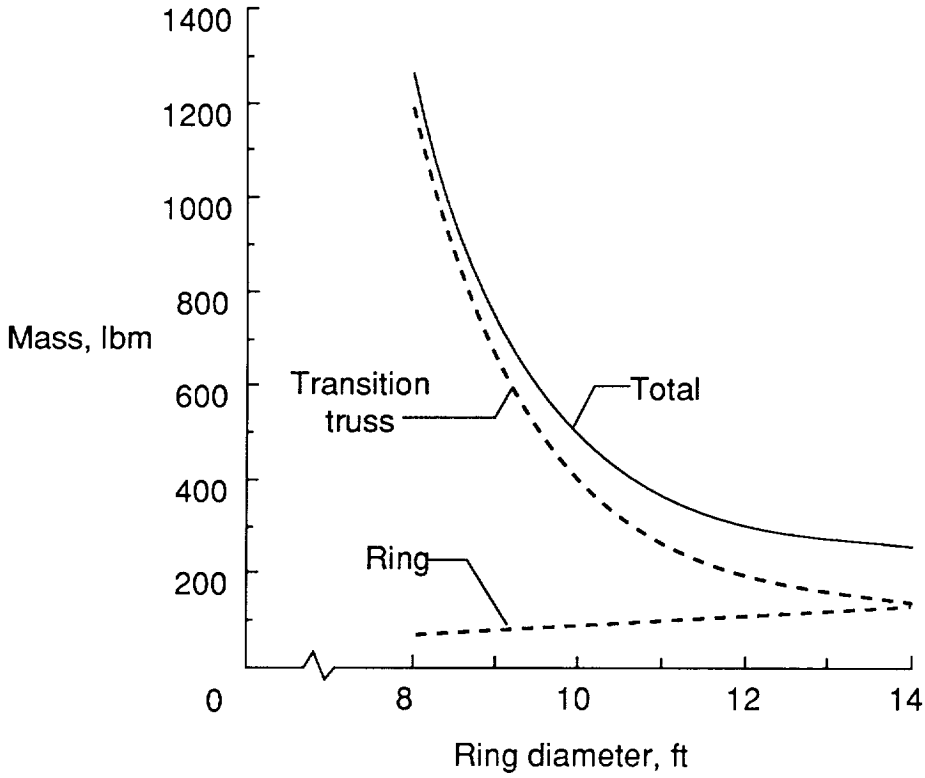

(a) One-bay joint.

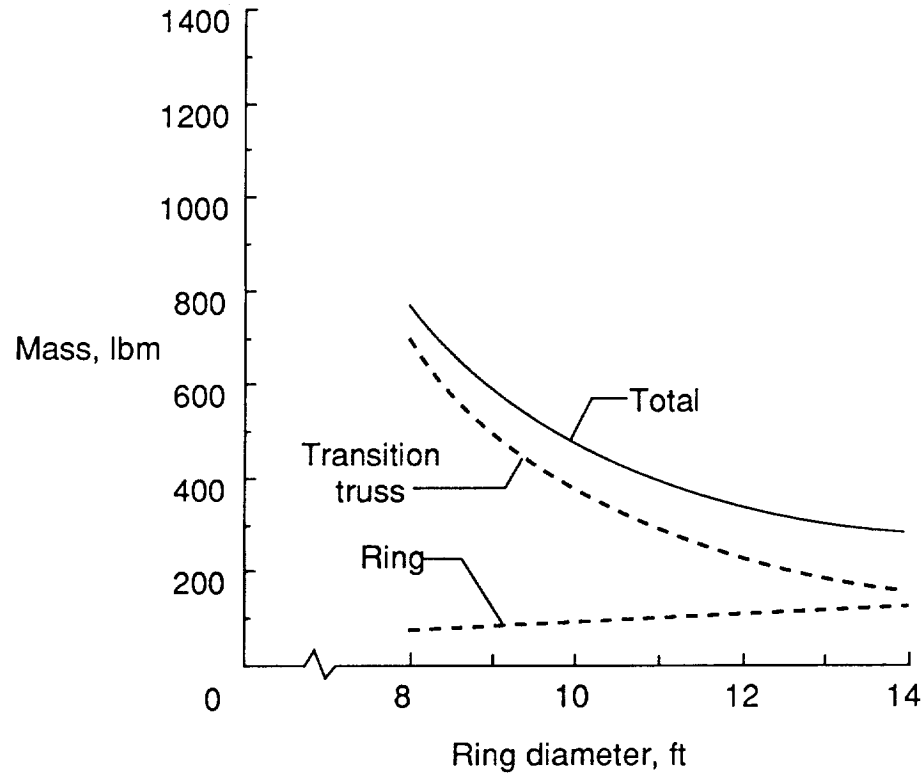

(b) Two-bay joint.

Figure 9. Mass versus ring diameter.

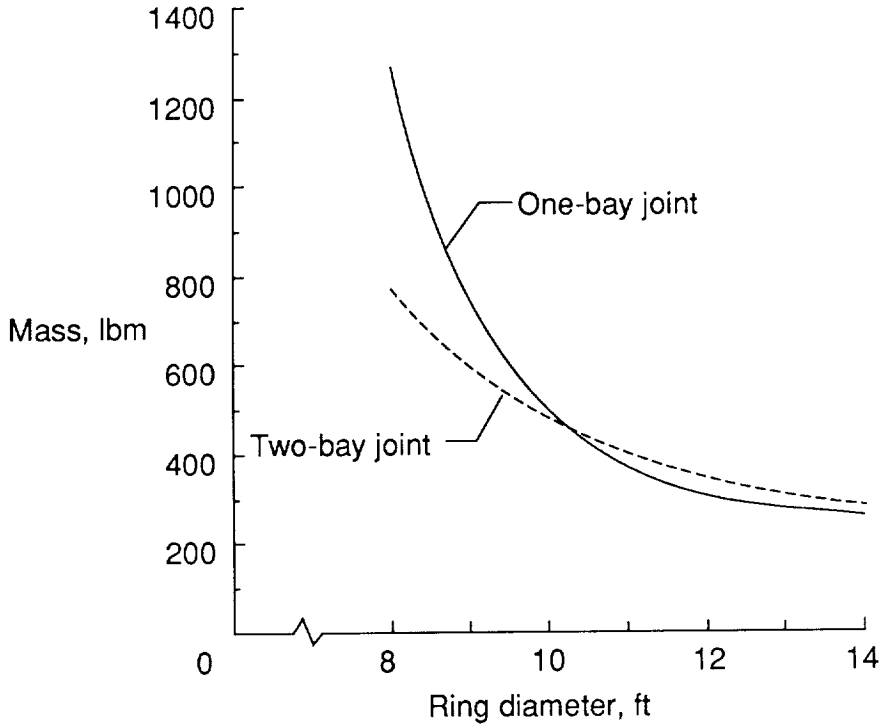

Figure 10. Comparison of structural mass of one- and two-bay joints.

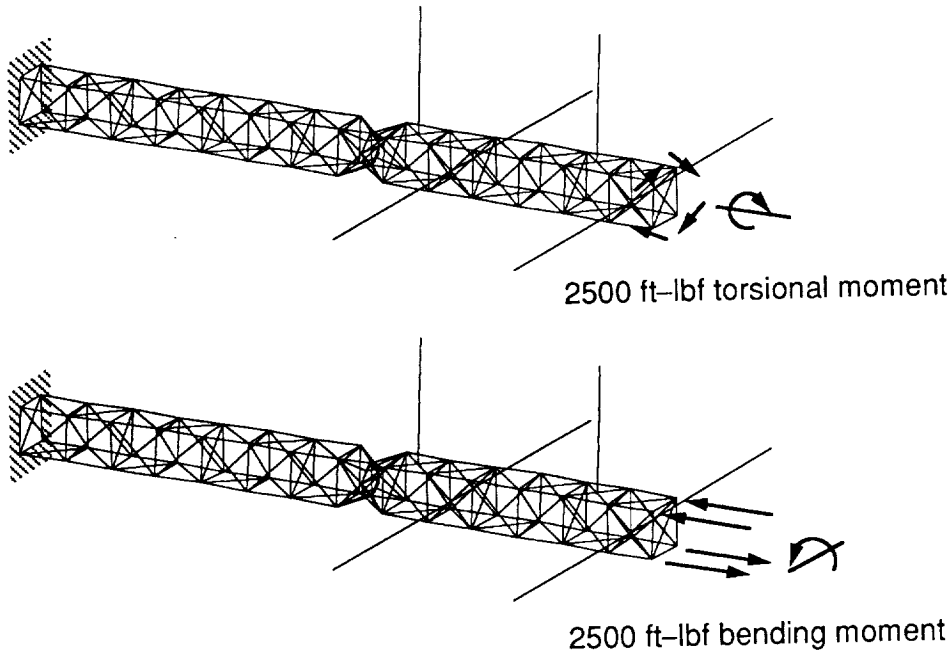

Figure 11. Static bending and torsional moments applied to truss.

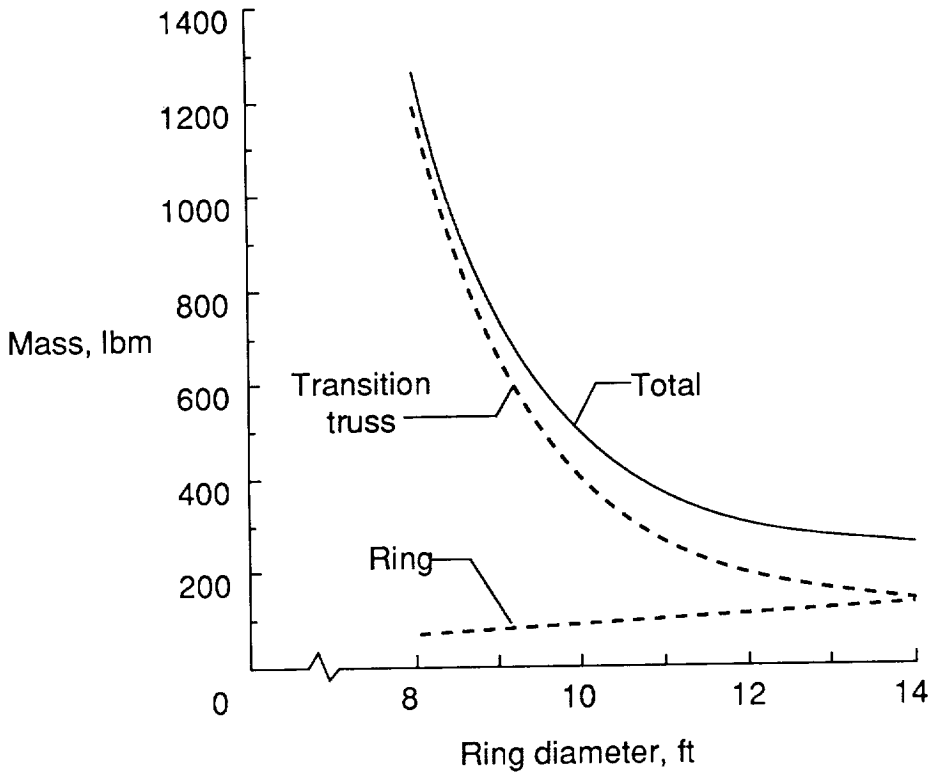

(a) One-bay joint.

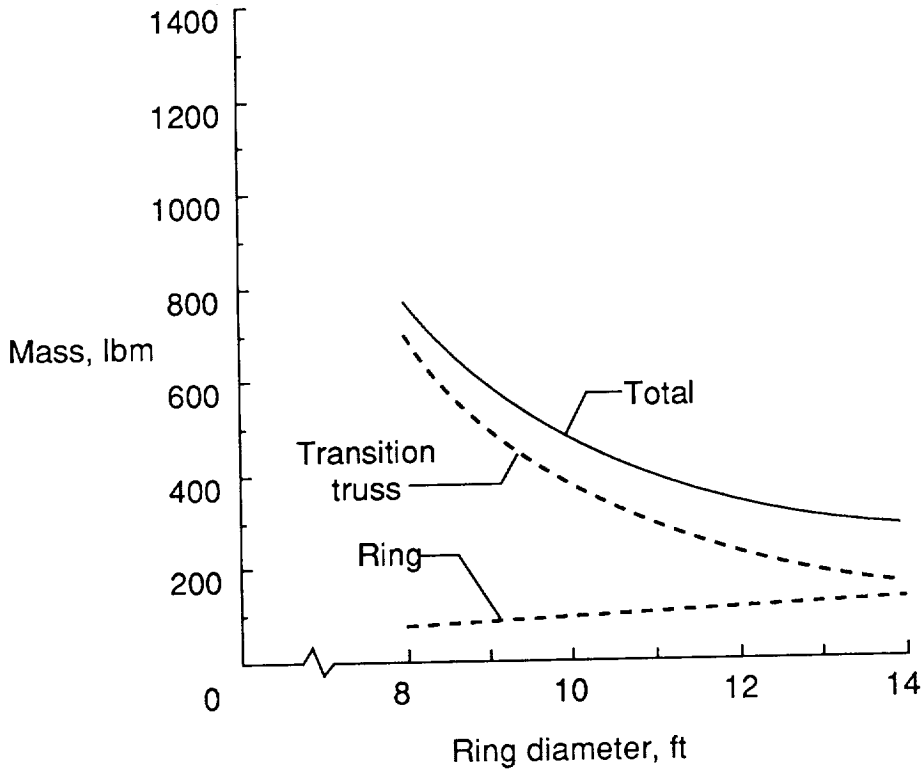

(b) Two-bay joint.

Figure 9. Mass versus ring diameter.

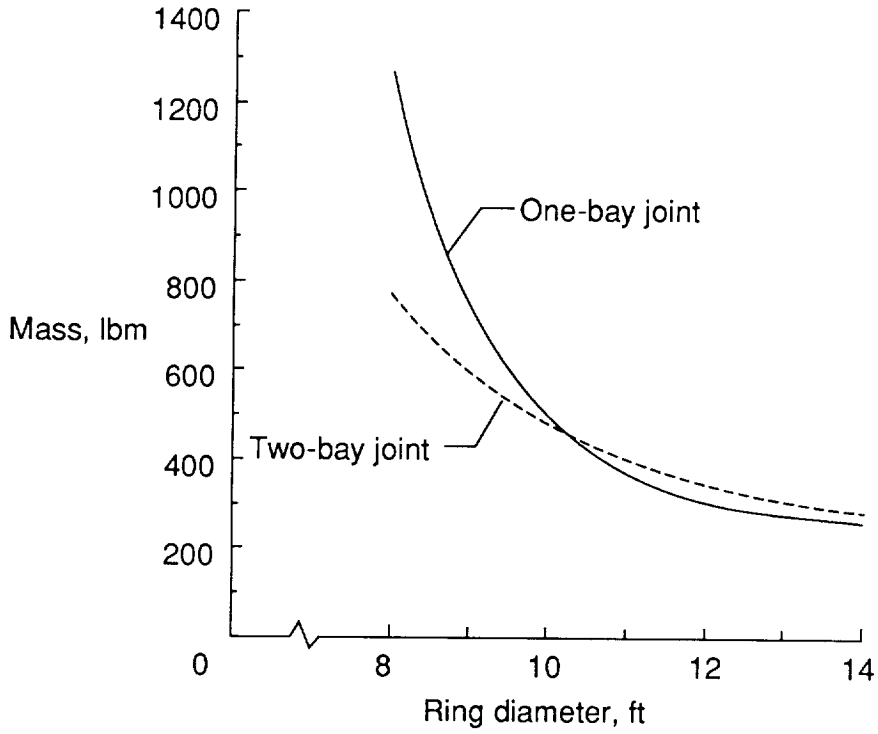

Figure 10. Comparison of structural mass of one- and two-bay joints.

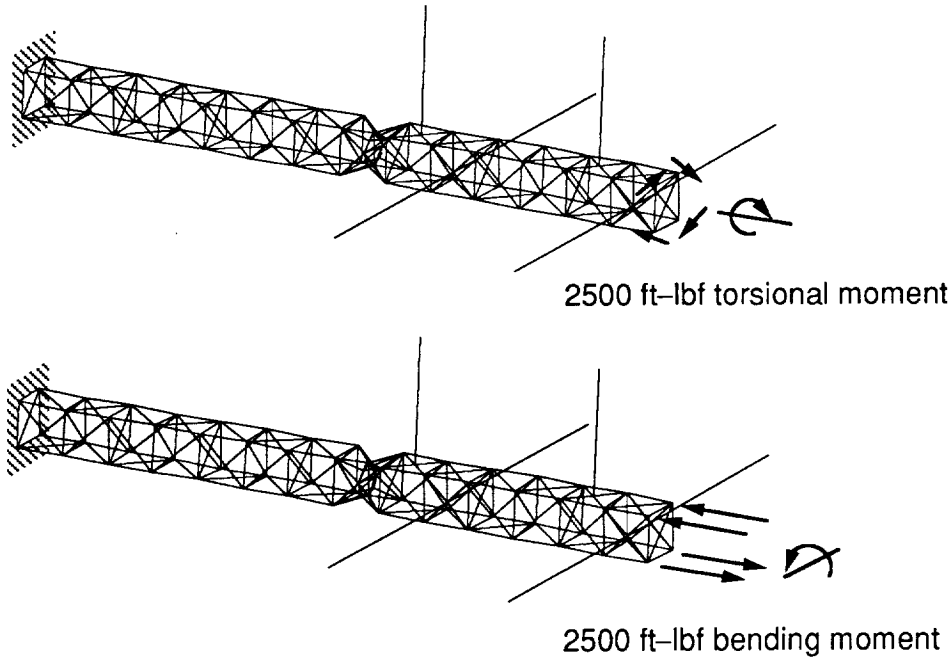

Figure 11. Static bending and torsional moments applied to truss.

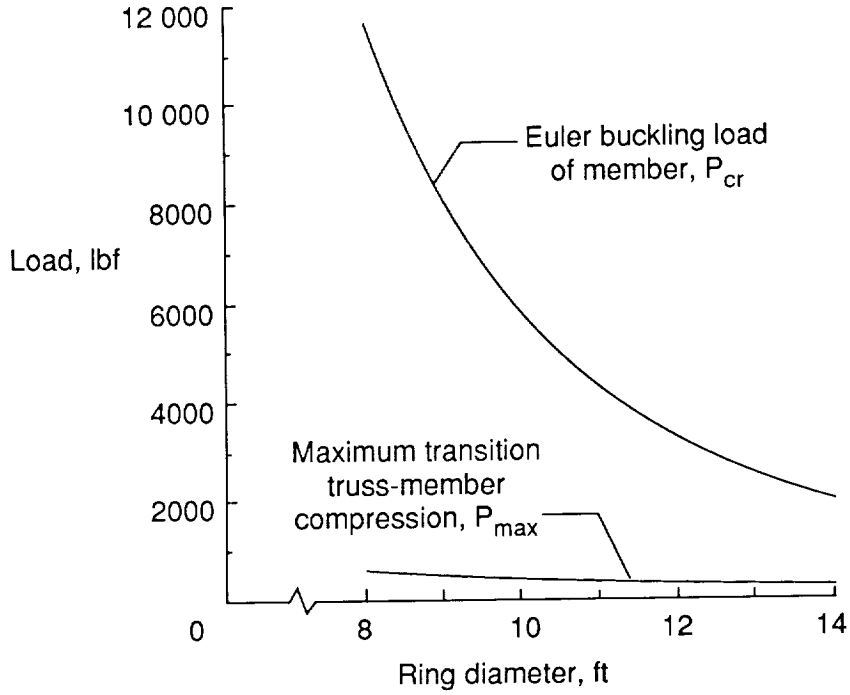

(a) Bending moment; one-bay joint.

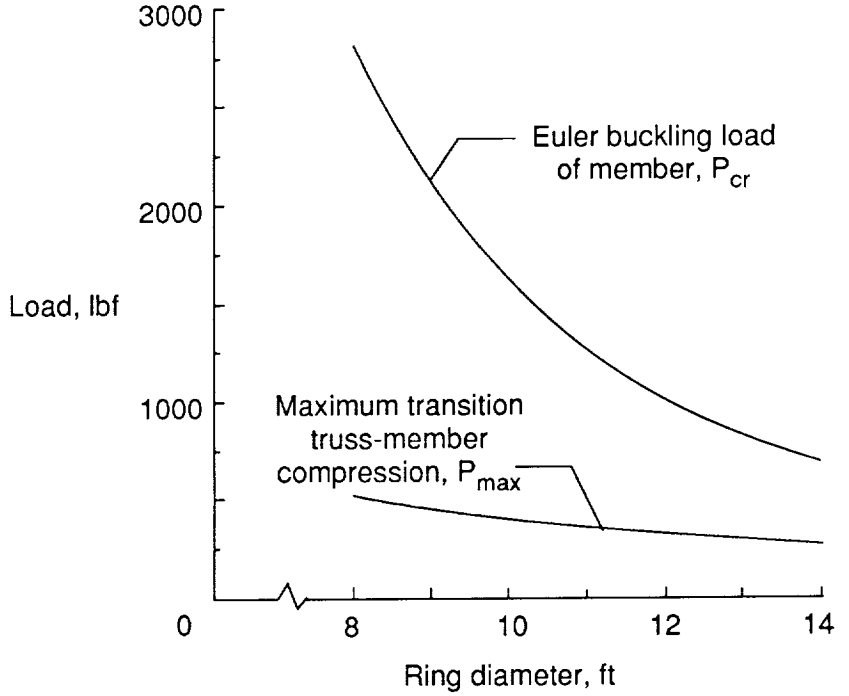

(b) Bending moment; two-bay joint.

Figure 12. Maximum transition truss-member load.

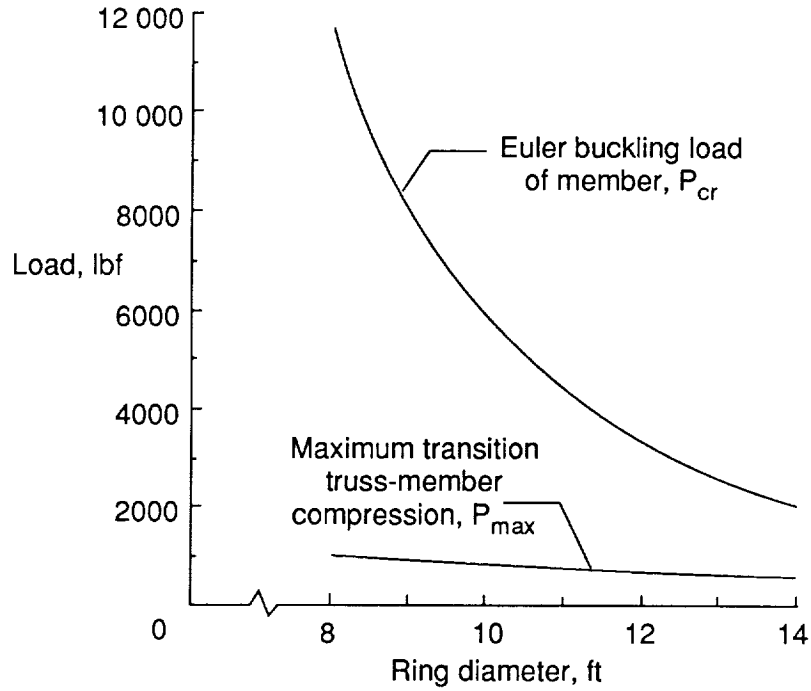

(c) Torsional moment; one-bay joint.

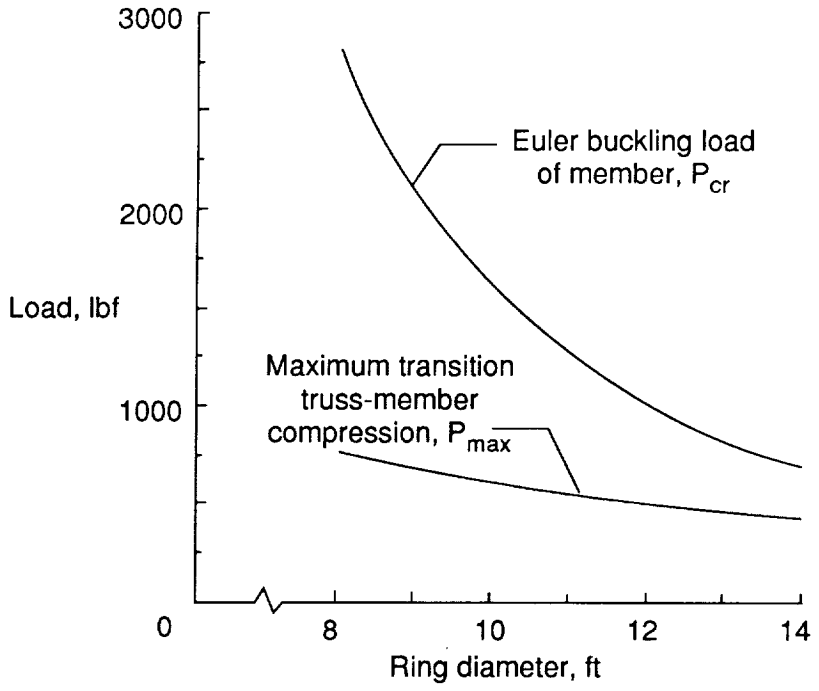

(d) Torsional moment; two-bay joint.

Figure 12. Concluded.

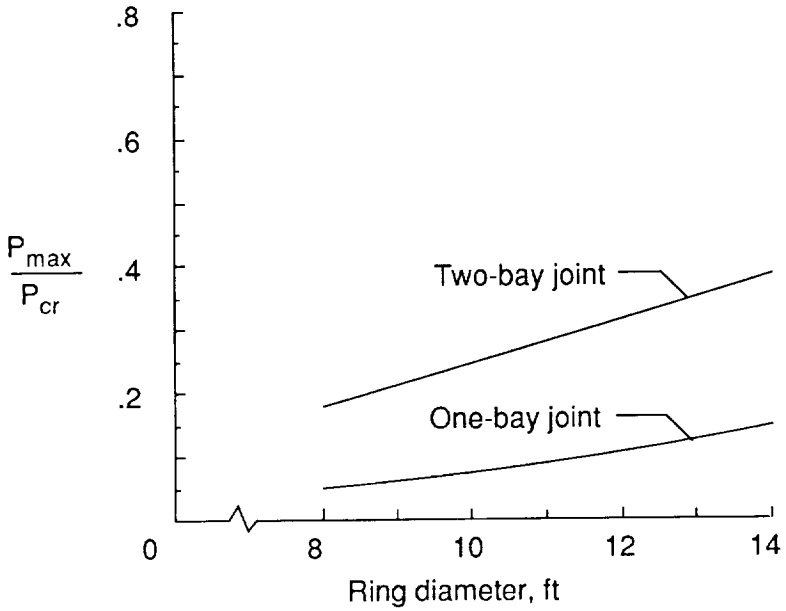

(a) Bending moment.

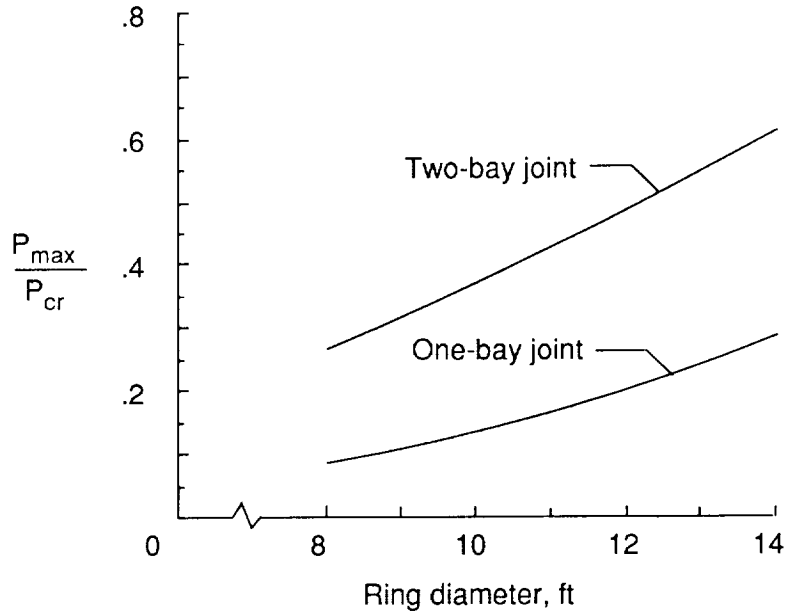

(b) Torsional moment.

Figure 13. Normalized maximum transition-truss member loads.

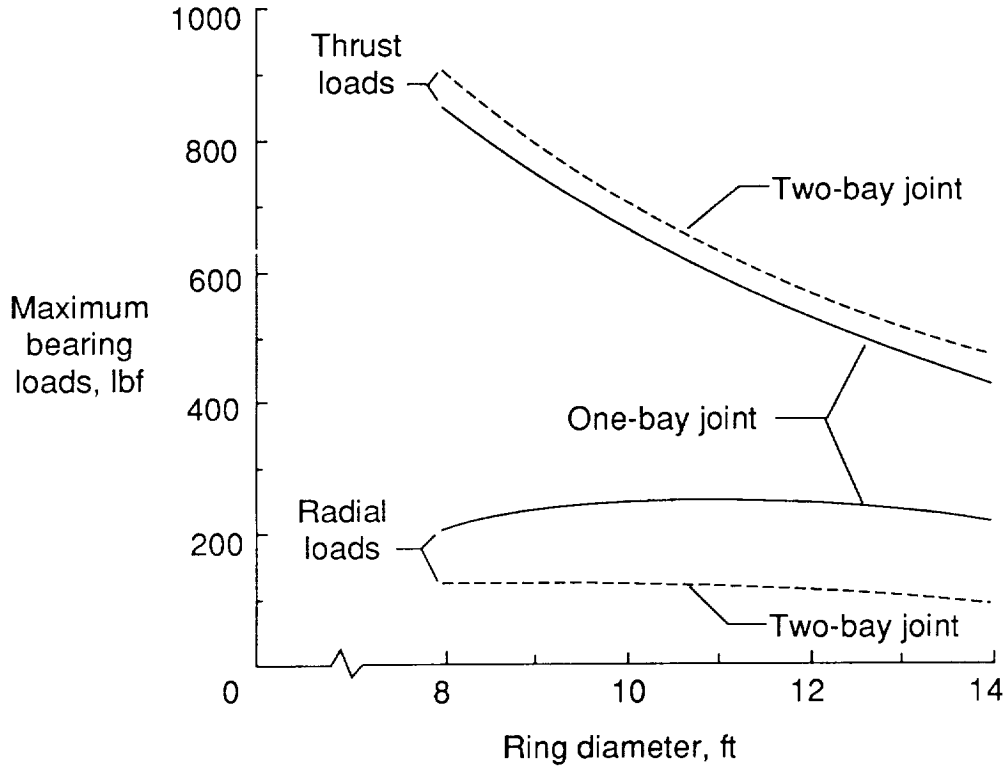

Figure 14. Maximum bearing loads for bending moment.